INDEPENDENT COMPONENT ANALYSIS (ICA) APPLIED TO LONG BUNCH BEAMS IN THE LOS ALAMOS PROTON STORAGE RING*

J. Kolski†, R. Macek, R. McCrady, X. Pang, LANL, Los Alamos, NM, 87545, USA

Abstract

Independent component analysis (ICA) is a powerful blind source separation (BSS) method [1]. Compared to the typical BSS method, principal component analysis (PCA), which is the BSS foundation of the well known model independent analysis (MIA) [2], ICA is more robust to noise, coupling, and nonlinearity [3, 4, 5]. ICA of turn-by-turn beam position data has been used to measure the transverse betatron phase and amplitude functions, dispersion function, linear coupling, sextupole strength, and nonlinear beam dynamics [3, 4, 5]. We apply ICA in a new way to slices along the bunch, discuss the source signals identified as betatron motion and longitudinal beam structure, and for betatron motion, compare the results of ICA and PCA.

INTRODUCTION

We apply ICA and PCA in a new way to slices along the bunch. We digitize sum and difference beam position signals for a full injection-extraction cycle, divide the digitized signal into time slices of equal length using the 0.5 ns digitization bin length, and stack the long digitized signal vector turn-by-turn to form the data matrix

$$\mathbf{x}(t) = \begin{pmatrix} x_1(1) & x_1(2) & \dots & x_1(N) \\ x_2(1) & x_2(2) & \dots & x_2(N) \\ \vdots & \vdots & \ddots & \vdots \\ x_M(1) & x_M(2) & \dots & x_M(N) \end{pmatrix}, \qquad (1)$$

such that each row of $\mathbf{x}$ is beam signal from a time slice.

ICA and PCA separate source signals from data without a model. The source signals from ICA and PCA are respectively independent and uncorrelated. Independence is a stronger mathematical property than uncorrelatedness. ICA and PCA model $\mathbf{x}$ as a linear combination of independent components (ICs) and principal components (PCs) respectively and yield respectively modes and patterns, describing the source signal's strength in space and time.

Introduction to PCA

The core of PCA is singular value decomposition (SVD). SVD of $\mathbf{x}$ yields eigenvectors $\mathbf{U}$, which span column-space (the space of slice number) and are called spatial patterns, and $\mathbf{V}$, which span in row-space (the space of turn number) and are called temporal patterns, connected by a diagonal matrix of singular values (SVs) $\mathbf{\Lambda}$ representing a PC's strength,

$$\mathbf{x}_{M\times N} = \mathbf{U}_{M\times M}\mathbf{\Lambda}_{M\times N}\mathbf{V}^T_{N\times N}. \qquad (2)$$

* Work supported by in part by United States Department of Energy under contract DE-AC52-06NA25396. LA-UR 12-21366 and 12-21411

† Electronic address: jkolski@lanl.gov

Introduction to ICA

ICA calculates L source signals $\mathbf{s}$ given $\mathbf{x}$, but the mixing matrix $\mathbf{A}$ is unknown

$$\mathbf{x}_{M\times N} = \mathbf{A}_{M\times L}\mathbf{s}_{L\times N}. \qquad (3)$$

For time series data, source signal independence is related to diagonality of covariance matrices [6]. We write the time-lagged source signal covariance matrix

$$\mathbf{C}_s(\tau) = \langle \mathbf{s}(t)\mathbf{s}(t-\tau)^T\rangle. \qquad (4)$$

First, $\mathbf{x}$ is preprocessed to obtain mean-zero ($\bar{\mathbf{x}} = \langle\mathbf{x}\rangle$), whitened data ($\mathbf{z}\mathbf{z}^T = \mathbf{I}$). SVs from SVD of $\bar{\mathbf{x}}$ are separated via a cutoff condition λ_c ($\mathbf{U}_1$, $\mathbf{\Lambda}_1 \geq \lambda_c$), and $\mathbf{z} = \mathbf{Y}\bar{\mathbf{x}} = \mathbf{\Lambda}_1^{-1/2}\mathbf{U}_1^T\bar{\mathbf{x}}$. Then, $\mathbf{C}_z(\tau_k)$ is calculated for a set of time lags (τ_k, $k = 0, 1, \dots, K$). Since the modified time-lagged covariance matrix $\bar{\mathbf{C}}_z(\tau_k) = \left(\mathbf{C}_z(\tau_k) + \mathbf{C}_z(\tau_k)^T\right)/2$ is real and symmetric, SVD is well defined,

$$\bar{\mathbf{C}}_z(\tau_k) = \mathbf{W}\mathbf{D}_k\mathbf{W}^T, \qquad (5)$$

where $\mathbf{W}$ is the unitary demixing matrix and $\mathbf{D}_k$ is a diagonal matrix. The Jacobi angle technique discussed in Ref. [7] is used to find the demixing matrix $\mathbf{W}$, which is a joint diagonalizer for all $\bar{\mathbf{C}}_z(\tau_k)$. $\mathbf{A}$ and $\mathbf{s}$ are calculated

$$\mathbf{A} = \mathbf{Y}^{-1}\mathbf{W} \quad \text{and} \quad \mathbf{s} = \mathbf{W}^T\mathbf{Y}\bar{\mathbf{x}}. \qquad (6)$$

INDEPENDENT COMPONENTS

ICs are presented in several graphs; see Fig. 1:

Top left spatial mode (blue), last turn beam profile (green).

Bottom left fft of spatial mode (top left), peak integer revolution harmonic, resolution $(1/1)$.

Top center integrated spatial mode (top left) (blue), last turn beam profile (green).

Bottom center correlation of IC and $\mathbf{z}(t-\tau)$, SV.

Top right temporal mode (-1 = last turn), fractional revolution harmonic from sinusoid fit.

Bottom right fft of temporal mode (top right), peak fractional revolution harmonic, resolution $(1/N)$.

Betatron ICs

In previous applications, ICA obtains quality ICs representing betatron motion [3, 4, 5], so the betatron IC result from slices along the bunch is of interest. We induce coherent betatron oscillation with a single-turn kick. The beam is stored for 420 turns (150 μs) after the kick.

The IC in Fig. 1 is identified as betatron motion because the fractional revolution harmonic (bottom right) is close to the operating fractional betatron tune value, 0.1805.

ISBN 978-3-95450-115-1

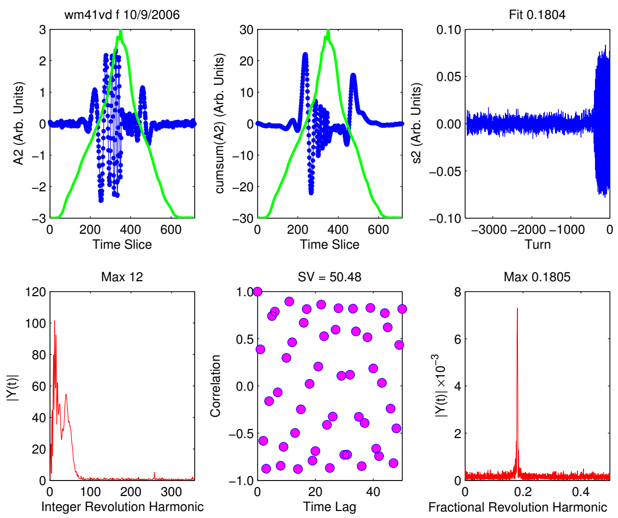

Figure 1: (Color) Typical betatron IC resulting from ICA of the difference signal for a single-turn kick.

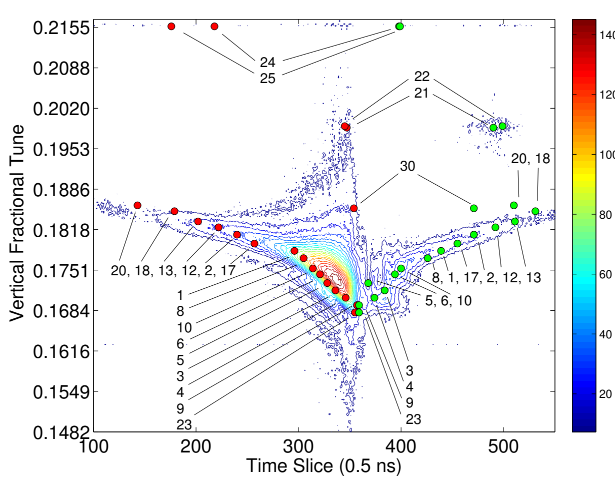

Figure 2: (Color) Betatron tune along the bunch and the greatest strength location for the first 30 ICs, some of which lie outside the plot boundary. The contour plots fft($\mathbf{x}$) along turn for each time slice. The red and green circles mark the leading and trailing edge greatest strength locations respectively with IC number indicated by numeric labels. The beam profile peak is located at time slice 350.

We wish to compare the betatron ICs with fft($\mathbf{x}$). We define the greatest strength location to be the fractional revolution harmonic and time slice where an IC is strongest. We calculate a leading and trailing edge greatest strength location for each IC and compare with fft($\mathbf{x}$) in Fig. 2. The betatron ICs' greatest strength locations reproduce fft($\mathbf{x}$). The spatial mode (top left) in Fig. 1 replicates the 0.1805 fractional tune portion along the bunch of fft($\mathbf{x}$) in Fig. 2. The betatron ICs must be viewed in concert as in Fig. 2 to obtain the full picture of the coherent space charge tune shift along the bunch.

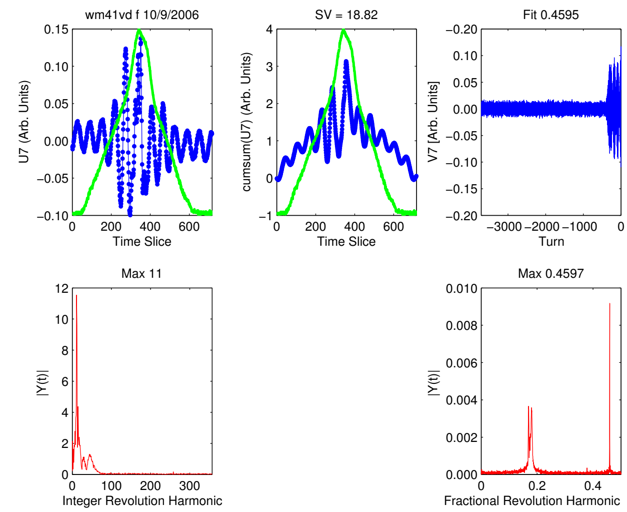

Figure 3: (Color) Typical betatron PC resulting from PCA of the difference signal for a single-turn kick.

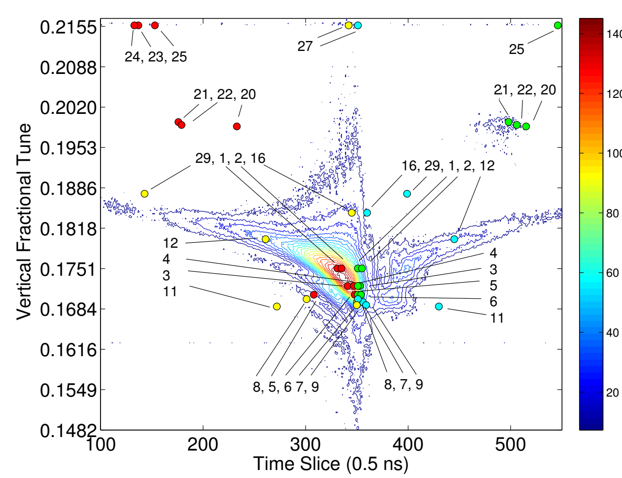

Figure 4: (Color) Betatron tune along the bunch and the greatest strength location for the first 30 PCs, some of which lie outside the plot boundary. The contour plots fft($\mathbf{x}$) along turn for each time slice. The red (yellow) and green (cyan) circles mark the leading and trailing edge greatest strength locations respectively for PCs with dominant betatron motion (dominant source signal other than betatron motion, like Fig. 3). A numeric label indicates PC number. The beam profile peak is located at time slice 350.

For comparison, we apply PCA to $\mathbf{x}$. The betatron PC plotted in Fig. 3 has dominant fractional revolution harmonic (bottom right) 0.46 and mixes with much of the tune distribution, indicated by the broad peak in the temporal pattern fft. The spatial pattern (top left) also exhibits mixing of source signals. The substance of this PC is corrupted by PCA's incomplete source separation.

We compare the PCA result with fft($\mathbf{x}$) in Fig. 4. Most betatron PCs have peak strengths located near the bunch

ISBN 978-3-95450-115-1

center where the difference signal is largest because PCA is unable to diagonalize the frequency continuum beyond its peak strength and average location. It is clear from Fig. 4 that PCA is unable to recover the coherent space charge tune shift along the bunch.

201.25 MHz IC

The 201.25 MHz IC represents the longitudinal structure of beam newly injected in the PSR, Fig. 5. The 201.25 MHz IC is identified by the character of its temporal mode (top right), which has constant amplitude for the first 1400 turns and suddenly reduces to noise for the last 500 turns. The reduction coincides with the end of accumulation.

The total revolution harmonic is 72.07136 as expected because the PSR design revolution frequency is the 72.07 subharmonic of the 201.25 MHz linac frequency. Multiplying the total revolution harmonic by the revolution frequency yields exactly 201.25 MHz.

At the beginning of the 2010 LANSCE production run cycle, we observed an unusual amount of "hash" noise-like structure on the PSR beam profile. ICA of the hashy beam signal yields the 201.25 MHz IC plotted in Fig. 6, which is reminiscent of Fig. 5 with obvious difference in the temporal mode (top right). A fractional revolution harmonic 0.009 describes an oscillation that repeats every 111 turns. The slow injection rastering causes the hashy beam profile by longitudinally stacking the beam upon itself more than in nominal operations where the fractional revolution harmonic is 0.07.

We calculate the PSR revolution frequency from the IC plotted in Fig. 6. The unchanging 201.25 MHz linac frequency is divided by the total revolution harmonic 72.009. This results in a revolution frequency of 2.7948 MHz. However, the PSR design revolution frequency is 2.7924 MHz. The revolution frequency differs from design by 2.4 kHz causing the hash on the current profile.

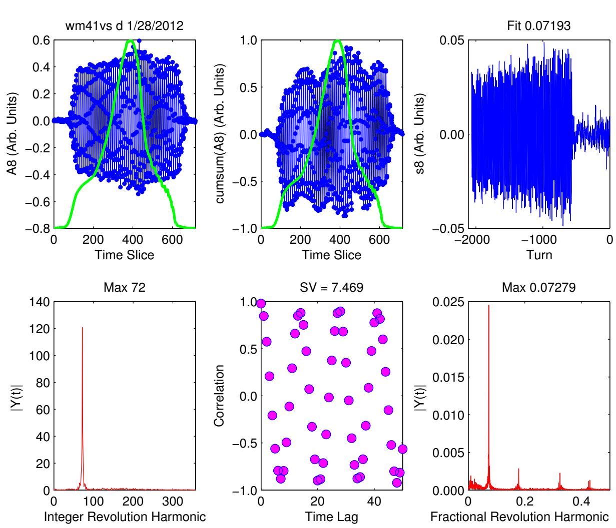

Figure 5: (Color) Typical 201.25 MHz IC resulting from ICA of the sum signal.

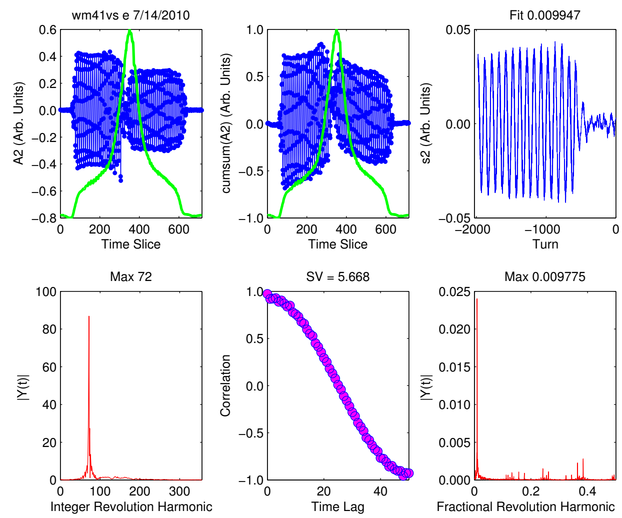

Figure 6: (Color) 201.25 MHz IC resulting from ICA of the sum signal when the revolution frequency is near an integer subharmonic of the linac frequency.

The PSR revolution frequency is created by a frequency generator into which a value is typed. For this run, the frequency generator value was inadvertently set to 2.7948 MHz; exactly the number predicted by ICA.

CONCLUSIONS

We adopt a new method applying ICA to slices along the beam and test with PSR sum and difference beam position signals digitized for an entire injection-extraction cycle.

We determine that PCA is inadequate for the BSS problem of slices along the bunch because PCA is unable to completely separate the source signals, yielding PCs describing a mixture of two or more source signals.

We discuss two classes of ICs, identified by spatial and temporal modes, describing betatron motion along the pulse and the longitudinal structure of newly injected beam.

REFERENCES

[1] A. Hyvärinen, et al., (John Wiley & Sons, New York, 2001).

[2] J. Irwin, et al., Phys. Rev. Lett. **82**, 1684 (1999); C.X. Wang, Ph.D. thesis, unpublished (Stanford University 1999).

[3] X. Huang, et al., PR-STAB **8**, 064001 (2005); X. Huang, Ph.D. thesis, unpublished (Indiana University 2005).

[4] F. Wang and S.Y. Lee, PR-STAB **11**, 050701, (2008); F. Wang, Ph.D. thesis, unpublished (Indiana University 2008).

[5] X. Pang and S.Y. Lee, Journal of Applied Physics, **106**, 074902 (2009); X. Pang, Ph.D. thesis, unpublished (Indiana University 2009).

[6] A. Belouchrani, et al., IEEE Trans. Signal Processing, **45**, 434-444, (1997).

[7] J.F. Cardoso and A. Souloumiac, SIAM J. Mat. Anal. Appl., **17**, 161, (1996).